

Topology and analysis of an N -stage cascaded polymer eight-port microring optical router with $7N$ channel wavelengths*

LI Cui-ting (李翠婷), ZHENG Ling-jiao (郑玲娇), ZHENG Yue (郑悦), and ZHENG Chuan-tao (郑传涛)**

State Key Laboratory on Integrated Optoelectronics, College of Electronic Science and Engineering, Jilin University, Changchun 130012, China

(Received 27 October 2014)

©Tianjin University of Technology and Springer-Verlag Berlin Heidelberg 2015

Eight-port optical routers are widely used in cluster-mesh photonic networks-on-chip (NoC). By using 24 groups of cross-coupling two-ring resonators, a 1-stage 8-port polymer optical router is proposed, which can optically route 7 channel wavelength data streams along definite path in two-dimensional (2D) plane. Under the selected 7 channel wavelengths, the insertion losses along all routing paths are within 0.02–0.58 dB, the maximum crosstalk of all routing operations is less than –39 dB, and the device footprint size is about 0.79 mm². Then, a universal novel structure and routing scheme of N -stage cascaded 8-port optical router are presented, which contains $7N$ channel wavelengths. Because of the good scalability in wavelength, this device shows potential application of wideband signal routing in optical NoC.

Document code: A **Article ID:** 1673-1905(2015)01-0036-5

DOI 10.1007/s11801-015-4204-1

In a chip multi-processor (CMP) based optical network-on-chip (NoC), a processor core should be capable of connecting with other processor cores, which can be realized by using an optical router located at each node of photonic NoC^[1-3]. Polymeric materials are widely used in the design and fabrication of optical devices^[4], and also the microring resonator (MRR) has become a preferable structure to construct optical waveguide components, such as filter, switch and modulator, due to its compact structure^[5]. Today, only 4-port and 5-port optical routers^[6-10] are not enough to construct all photonic NoCs. High-radix non-blocking optical routers with even more ports possess potential applications in the future on-chip optical interconnects.

In this paper, by using polymer materials, we propose a kind of 8-port passive microring optical router for photonic NoC application, and 7 channel wavelengths spaced by 0.8 nm are included, which can route an optical signal from one port to its definite port according to the wavelength. The ring waveguide structure has already been used in our previous design on 4-port and 5-port passive optical routers^[11,12]. In this paper, by cascading the 1-stage 8-port optical router, a universal structure of N -stage 8-port optical router is constructed, which can optically route $7N$ channel wavelengths between all input ports and all output ports, and along each

port-to-port data link, N channel wavelengths are included. The scalability in routing channel wavelength of this device structure is an obvious contribution of this paper, which broadens the application of such a router in NoC systems. Therefore, after serial cascading on the basic 8-port optical router, the proposed device becomes a wideband optical router for standard wavelength division multiplexing (WDM) signal routing.

The structure model of the designed 8-port polymer optical router is shown in Fig.1(a), which consists of 7 channel waveguides and 24 groups of cross-coupling two-microring resonators with 6 kinds of ring radii corresponding to 6 kinds of resonance wavelengths, and the structure of the polymer cross-coupling two-microring resonator is shown in Fig.1(b). The two waveguide lines marked by I_i and O_i ($i=0-7$) belong to one port. The length of input and output waveguide of each port is $L_1=100\ \mu\text{m}$, and the center to center space of two neighboring rings is designed to be $L_2=100\ \mu\text{m}$. Four circular bending waveguides with bending radii of R_{c1} , R_{c2} , R_{c3} and R_{c4} are also adopted in the topology, and their waveguide lengths are L_{d1} and L_{d2} , respectively.

The cross-section view over the coupling plane between MRR waveguide and channel waveguide is shown in Fig.1(c). Around 1550 nm, the refractive indices of the polymer waveguide core^[13], the polymer buffer

* This work has been supported by the National Natural Science Foundation of China (Nos.61107021, 61177027 and 61077041), the Ministry of Education of China (Nos.20110061120052 and 20120061130008), the China Postdoctoral Science Foundation Funded Project (Nos. 20110491299 and 2012T50297), the Science and Technology Department of Jilin Province of China (No.20130522161JH), and the Special Funds of Basic Science and Technology of Jilin University (No.201103076).

** E-mail: zhengchuantao578@163.com

layer^[14] and the left/right cladding (air) are $n_{10}=1.590$, $n_{20}=1.461$ and $n_{30}=1.000$, respectively, and their bulk amplitude attenuation coefficients are $\alpha_{10}=0.25$ dB/cm, $\alpha_{20}=0.25$ dB/cm and $\alpha_{30}=0$, respectively. In the design, E_{00}^y is selected as the fundamental propagation mode.

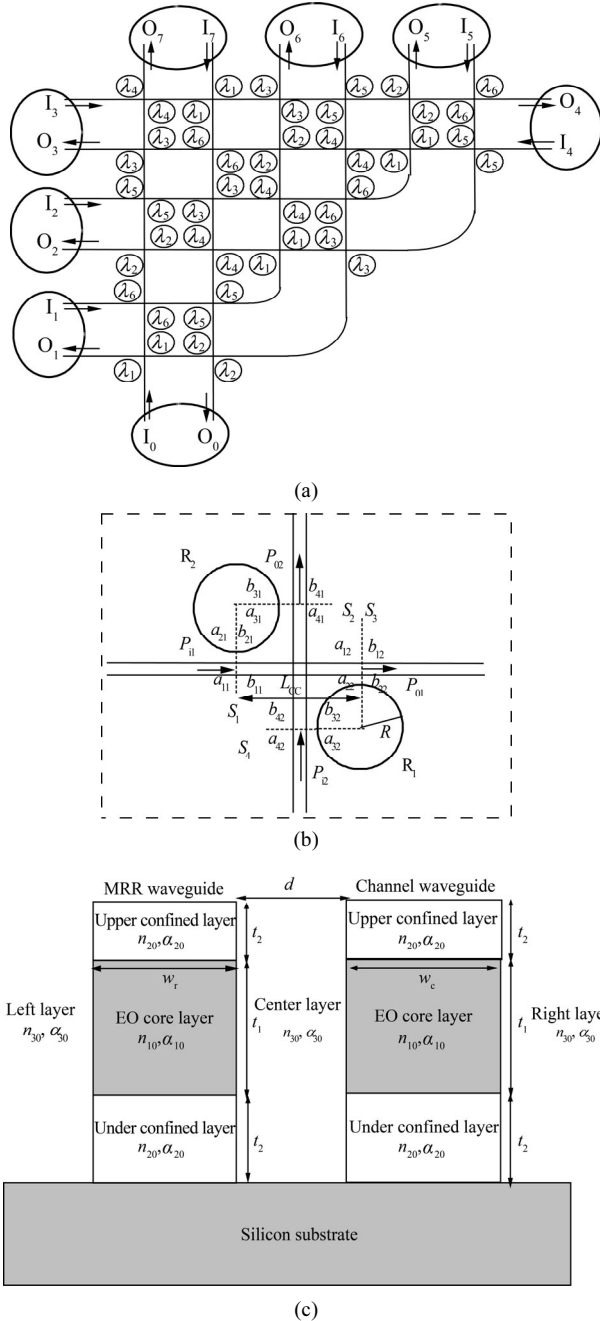


Fig.1 (a) Structure of the one-stage polymer 8-port optical router; (b) Structure of the polymer cross-coupling two-microring resonator; (c) Cross-section view over the coupling region between MRR waveguide and channel waveguide

Without considering the bending effect of MRR waveguide, the mode characteristics of the rectangular waveguide can be analyzed by using the theoretical approach proposed in Ref.[15]. Under the case of consid-

ering the bending effect, those of the curved rectangular waveguide can be analyzed with the numerical approach proposed in Ref.[16]. The programs based on Matlab are compiled for solving the effective refractive index of each order mode. In order to realize single-mode propagation and obtain the same mode propagation constants between MRR waveguide and channel waveguide, the waveguide parameters at 1550 nm are optimized as listed in Tab.1. Detailed optimization process can be seen in Ref.[17].

Tab.1 Optimized parameters of the basic cross-coupling MRR at 1550 nm

Parameter	Optimum values
Core thickness t_1	1.7 μm
Core width w_c	2.03 μm
Core width w_r	1.7 μm
Buffer thickness t_2	2.5 μm
Resonance order m	85
Coupling gap d	0.14 μm
Transmittance coefficient t_{CR}	0.996 22
Coupling coefficient κ_{CR}	0.086 84
Channel waveguide mode effective index n_C	1.524 3
Ring waveguide mode effective index n_R	1.524 3
Channel waveguide mode loss coefficient α_C	0.256 2 dB/cm
Ring waveguide mode loss coefficient α_R	0.256 1 dB/cm

The designed 8-port optical router is operated under 7 kinds of wavelengths, and here 7 wavelengths satisfying standard WDM wavelength spacing of 0.8 nm are selected. Accordingly, the 8-port device requires 6 kinds of basic routing elements. Using the same way in Refs.[11] and [12], the resonance wavelengths and corresponding bending radii of the 6 kinds of microrings are listed in Tab.2.

Tab.2 The 7 selected routing wavelengths and 6 ring radii for the 1-stage 8-port optical router

Channel number	Channel wavelength (nm)	Ring radius (μm)	Mode effective index
1	1 548.4	13.740	1.524 47
2	1 549.2	13.748	1.524 39
3	1 550.0	13.756	1.524 31
4	1 550.8	13.764	1.524 23
5	1 551.6	13.772	1.524 15
6	1 552.4	13.780	1.524 07
7	1 553.2	/	/

When seven lightwave signals with wavelengths of $\lambda_1-\lambda_7$ are input into one certain port simultaneously, they can be output from their own appointed ports, which is called definite-path routing. For example, when the hy-

brid signal is input into port I_0 , according to the routing path marked in Fig.2, the seven signals with wavelengths of λ_1 – λ_7 will be output from ports O_1 – O_7 , respectively. All the possible definite-path routing links are shown in Tab.3.

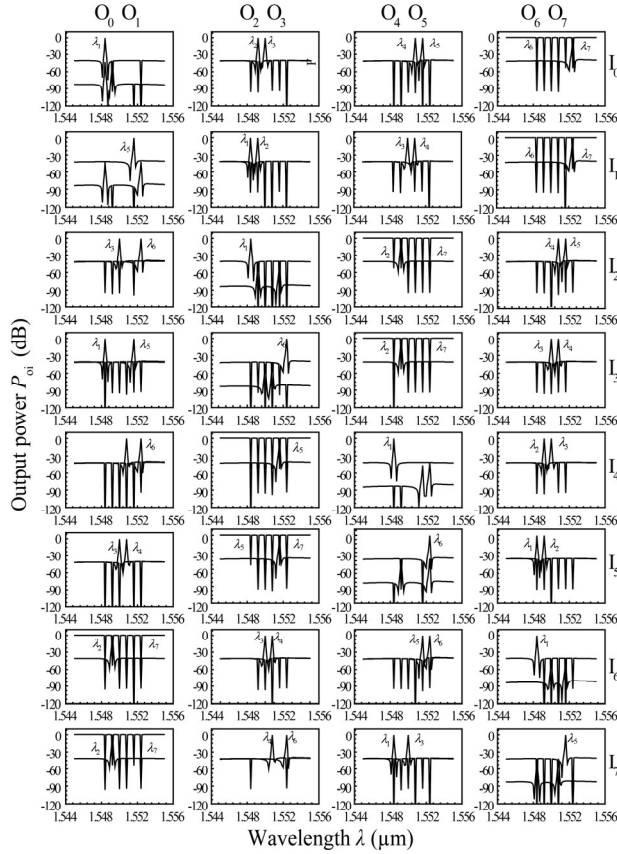


Fig.2 Optical spectral responses of 56 routing paths of the 1-stage 8-port optical router under different input/output routing operations

Tab.3 Routing paths of the 1-stage 8-port optical router

	Output							
	O_0	O_1	O_2	O_3	O_4	O_5	O_6	O_7
I_0	/	λ_1	λ_2	λ_3	λ_4	λ_5	λ_6	λ_7
I_1	λ_5	/	λ_1	λ_2	λ_3	λ_4	λ_7	λ_6
I_2	λ_3	λ_6	/	λ_1	λ_2	λ_7	λ_4	λ_5
Input	I_3	λ_1	λ_5	λ_6	/	λ_7	λ_2	λ_3
I_4	λ_6	λ_4	λ_5	λ_7	/	λ_1	λ_2	λ_3
I_5	λ_4	λ_3	λ_7	λ_5	λ_6	/	λ_1	λ_2
I_6	λ_2	λ_7	λ_3	λ_4	λ_5	λ_6	/	λ_1
I_7	λ_7	λ_2	λ_4	λ_6	λ_1	λ_3	λ_5	/

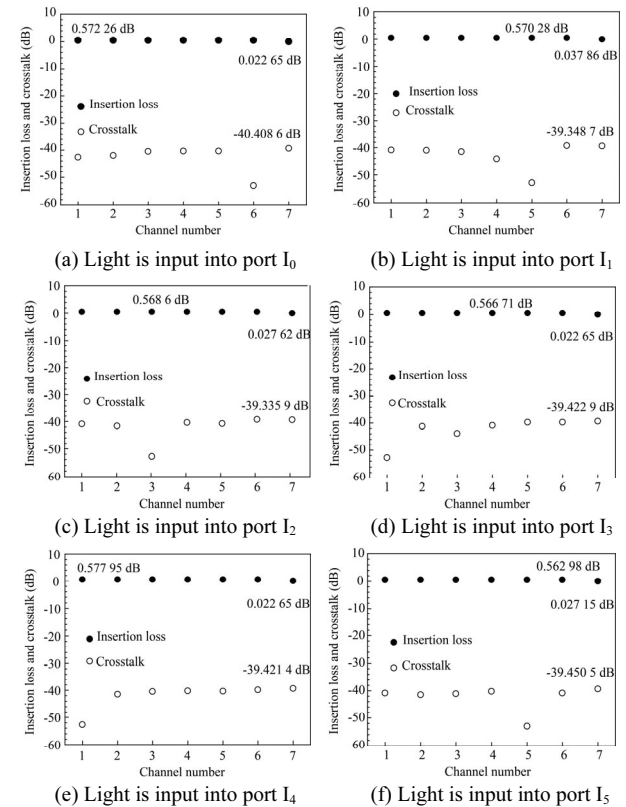
When a channel wavelength λ_k is input into port I_i , it will be output from an appointed port O_j ($i \neq j$), and we denote the routing path by I_i^j . The routing path from input port I_i to output port O_j is selected as the path with the nearest propagation distance, marked by I_i^j . During

the propagation of the light with wavelength λ from input port I_i to output port O_j , along the definite routing path I_i^j , it will pass through several basic routing elements (drop-state or through-state) and definitely long channel waveguide (with length of L_i^j), and for the basic routing unit with resonance wavelength λ_k ($k=1-7$), it is assumed that there are totally m_k drop-states with output power of $P_D^{\lambda_k}$ and n_k through-states with output power of $P_B^{\lambda_k}$. Therefore, the output powers in decibel form can be expressed as

$$P_i^j(\lambda) = -L_i^j \cdot 2\alpha_c(\lambda) + \sum_{k=1}^6 [m_k P_D^{\lambda_k}(\lambda) + n_k P_B^{\lambda_k}(\lambda)]. \quad (1)$$

Using Eq.(1), along each path, the output spectra of all output ports relative to each input port are calculated and shown in Fig.2.

Insertion loss and crosstalk are the intrinsic characteristics of photonic devices. We calculate the insertion losses under the cases of light being input into different ports and being output from the appointed ports (on-port), and calculate the crosstalks of all channel wavelengths under the cases of lightwave signals being input into different ports, as depicted in Fig.3. It can be found that the insertion losses of all channel wavelengths are approximately uniform, whose maximum value is 0.58 dB and minimum value is 0.02 dB, and the maximum crosstalks for all channel wavelengths are found to be less than -40.408 6 dB, -39.348 7 dB, -39.335 9 dB, -39.422 9 dB, -39.421 4 dB, -39.450 5 dB, -39.433 2 dB and -39.451 98 dB, respectively. We roughly calculate that the footprint size is about 0.79 mm².



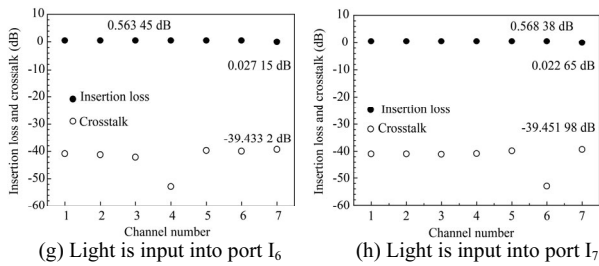


Fig.3 For the 1-stage 8-port optical router, the insertion losses of definite routing port and the crosstalks of this on-port relative to other off-ports, where the light is launching into ports I_0-I_6

Then we construct the universal structure of an N -stage 8-port optical router. For realizing the cascading between two neighboring 8-port routers without any waveguide crossing, we propose an equivalent 8-port optical router, whose topology is the second stage of the N -stage cascaded 8-port optical router as shown in Fig.4. For the convenient statement, we name the router in Fig.2 as ordinary router (OR), while name the router used as the second stage of the N -stage cascaded 8-port optical router shown in Fig.4 as unordinary router (UR).

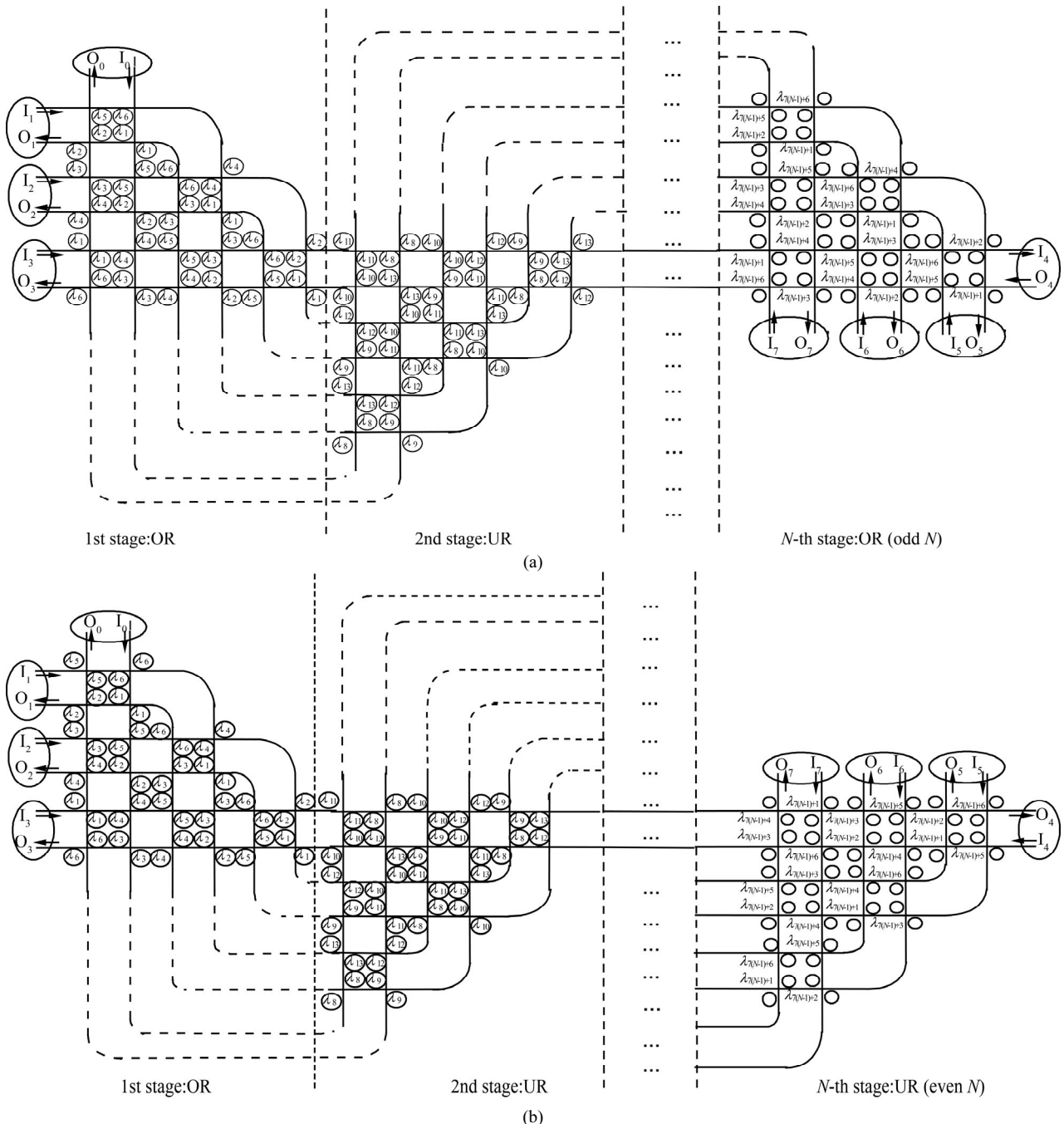


Fig.4 Structure of the N -stage cascaded 8-port optical router with $7N$ channel wavelengths, where (a) N is odd, and (b) N is even

In order to route more than seven wavelengths, the universal scheme of N -stage cascaded optical router with 8 ports and $7N$ channel wavelengths is proposed, where an OR is used in the odd stage and a UR is used in the even stage, as depicted in Fig.4(a) for an odd N and Fig.4(b) for an even N . The dash lines indicate the connection waveguides between the two stages, and there is no crossing by using an OR and a UR. For an odd N , there are $(N+1)/2$ ORs and $(N-1)/2$ URs, while for an even N , there are $N/2$ ORs and $N/2$ URs. The cascaded connection rule between the former stage and the latter stage is that the input/output ports $I_4, O_4, I_5, O_5, I_6, O_6, I_7$ and O_7 of the former stage connect with the input/output ports $O_3, I_3, O_2, I_2, O_1, I_1, O_0$ and I_0 of the latter stage, respectively. The i th stage contains seven channel wavelengths, which are labeled by $\lambda_{7(i-1)+1}, \lambda_{7(i-1)+2}, \lambda_{7(i-1)+3}, \lambda_{7(i-1)+4}, \lambda_{7(i-1)+5}, \lambda_{7(i-1)+6}$ and $\lambda_{7(i-1)+7}$, respectively. The wavelengths routed by all definite-path data-links are listed in Tab.4, where $i=1, 2, \dots, N$. Each data-link contains N channel wavelengths, and there are totally $7N$ channel wavelengths routed by the device. It should also be noted that in each stage, according to the wavelength number, from small to large, there is a distribution order of the 24 two-ring resonators. Based on the selected stage number, one can place the rings of the odd stage and even stage according to the rules shown in Fig.4.

Tab.4 Routing wavelength assignment of the N -stage 8-port optical router with scalable $7N$ channel wavelengths

	Output							
	O_0	O_1	O_2	O_3	O_4	O_5	O_6	O_7
I_0	/	λ_{i1}	λ_{i2}	λ_{i3}	λ_{i4}	λ_{i5}	λ_{i6}	λ_{i7}
I_1	λ_{i5}	/	λ_{i1}	λ_{i2}	λ_{i3}	λ_{i4}	λ_{i7}	λ_{i6}
I_2	λ_{i3}	λ_{i6}	/	λ_{i1}	λ_{i2}	λ_{i7}	λ_{i4}	λ_{i5}
Input	I_3	λ_{i1}	λ_{i5}	λ_{i6}	/	λ_{i7}	λ_{i2}	λ_{i3}
	I_4	λ_{i6}	λ_{i4}	λ_{i5}	λ_{i7}	/	λ_{i1}	λ_{i2}
	I_5	λ_{i4}	λ_{i3}	λ_{i7}	λ_{i5}	λ_{i6}	/	λ_{i1}
	I_6	λ_{i2}	λ_{i7}	λ_{i3}	λ_{i4}	λ_{i5}	λ_{i6}	/
	I_7	λ_{i7}	λ_{i2}	λ_{i4}	λ_{i6}	λ_{i1}	λ_{i3}	λ_{i5}

In conclusion, we firstly propose the 1-stage 8-port polymer optical router consisting of 6 cross-coupling MRRs, and the proper structural parameters are selected through optimization. It can route 7 channel wavelengths and includes 56 possible I/O routing paths. The insertion losses of all channel wavelengths along all routing paths are in the range of 0.02–0.58 dB, the maximum crosstalk between the on-port along each routing path and other off-ports is less than -39.335 9 dB, and the device has a footprint size of about 0.79 mm². Then a universal structure of N -stage 8-port optical router with scalable $7N$ channel wavelengths is constructed, which is a promising candidate for wideband signal routing operations in next-generation optical NoCs. The design scheme can

also be used to design other 8-port optical routers with any wavelength band according to the practical need.

References

[1] A. Joshi, C. Batten, K. Yong-Jin, S. Beamer, I. Shamim, K. Asanovic and V. Stojanovic, Silicon-Photonic Clos Networks for Global On-Chip Communication, 3rd ACM/IEEE International Symposium on Networks-on-Chip, 124 (2009).

[2] K. H. Mo, Y. Y. Ye, X. W. Wu, W. Zhang, W. C. Liu and J. Xu, A Hierarchical Hybrid Optical-Electronic Network-On-Chip, IEEE Computer Society Annual Symposium on VLSI, 327 (2010).

[3] M. Haurylau, G. Chen, H. Chen, J. Zhang, N. A. Nelson, D. H. Albonesi, E. G. Friedman and P. M. Fauchet, IEEE Journal on Selected Topics in Quantum Electronics **12**, 1699 (2006).

[4] J. Hong, Y. Liu and W. Chen, Journal of Optoelectronics-Laser **25**, 1668 (2014). (in Chinese)

[5] L. Liang, C. T. Zheng, Q. Song, C. S. Ma and D. M. Zhang, Journal of Optoelectronics-Laser **24**, 655 (2013). (in Chinese)

[6] M. Yang, W. M. J. Green, S. Assefa, J. Van Campenhout, B. G. Lee, C. V. Jahnes, F. E. Doany, C. L. Schow, J. A. Kash and Y. A. Vlasov, Optics Express **19**, 47 (2011).

[7] N. Sherwood-Droz, H. Wang, L. Chen, B. G. Lee, A. Biberman, K. Bergman and M. Lipson, Optics Express **16**, 15915 (2008).

[8] R. Ji, L. Yang, L. Zhang, Y. Tian, J. Ding, H. Chen, Y. Lu, P. Zhou and W. Zhu, Optics Express **19**, 18945 (2011).

[9] Y. Y. Ye, X. W. Wu, J. Xu, W. Zhang, M. Nikdast and X. Wang, Holistic Comparison of Optical Routers for Chip Multiprocessors, in Anti-Counterfeiting, International Conference on Anti-Counterfeiting, Security and Identification, 1 (2012).

[10] R. Ji, L. Yang, L. Zhang, Y. Tian, J. Ding, H. Chen, Y. Lu, P. Zhou and W. Zhu, Optics Express **19**, 20258 (2011).

[11] Q. Q. Luo, C. T. Zheng, X. L. Huang, Y. D. Wang and D. M. Zhang, Optical and Quantum Electronics **46**, 829 (2014).

[12] C. T. Zheng, Q. Q. Luo, C. S. Ma, D. M. Zhang and Z. B. Li, Optics Communications **322**, 214 (2014).

[13] G. Y. Xu, Z. F. Liu, J. Ma, B. Y. Liu, S. T. Ho, L. Wang, P. W. Zhu, T. J. Marks, J. D. Luo and A. K. Y. Jen, Optics Express **13**, 7380 (2005).

[14] C. Pitois, S. Vukmirovic, A. Hult, D. Wiesmann and M. Robertsson, Macromolecules **32**, 2903 (1999).

[15] E. A. J. Marcatili, Bell System Technical Journal **48**, 2071 (1969).

[16] A. Melloni, F. Carniel, R. Costa and M. Martinelli, Journal of Lightwave Technology **19**, 571 (2001).

[17] C. T. Zheng, L. Liang, Q. Q. Luo, C. S. Ma, D. M. Zhang and Y. D. Wang, IEEE Photonics Journal **5**, 7200620 (2013).